



Published in final edited form as:

*Int Urogynecol J.* 2023 August ; 34(8): 1923–1931. doi:10.1007/s00192-023-05482-9.

## Variations in structural support site failure patterns by prolapse size on stress 3D MRI

Christopher X. HONG, MD<sup>1</sup>, Ms. Lahari NANDIKANTI, BS<sup>2</sup>, Ms. Beth SHROSBREE, BS<sup>2</sup>, John O.L. DELANCEY, MD<sup>1</sup>, Luyun CHEN, PhD<sup>1,3</sup>

<sup>1</sup>Department of Obstetrics and Gynecology, University of Michigan, Ann Arbor, MI

<sup>2</sup>University of Michigan Medical School, University of Michigan, Ann Arbor, MI

<sup>3</sup>Department of Biomedical Engineering, University of Michigan

### Abstract

**Introduction and Hypothesis**—Our objective was to develop a standardized measurement system to evaluate structural support site failures among women with anterior vaginal wall-predominant prolapse according to increasing prolapse size using stress three-dimensional (3D) magnetic resonance imaging (MRI).

**Methods**—Ninety-one women with anterior vaginal wall-predominant prolapse and uterus *in situ* who had undergone research stress 3D MRI were included for analysis. The vaginal wall length and width, apex and paravaginal locations, urogenital hiatus diameter, and prolapse size were measured at maximal Valsalva on MRI. Subject measurements were compared to established measurements in 30 normal controls without prolapse using a standardized *z*-score measurement system. A *z*-score greater than 1.28, or the 90<sup>th</sup> percentile in controls, was considered abnormal. The frequency and severity of structural support site failure was analyzed based on tertiles of prolapse size.

**Results**—Substantial variability in support site failure pattern and severity was identified, even between women with the same stage and similar size prolapse. Overall, the most common failed support sites were straining hiatal diameter (91%) and paravaginal location (92%), followed by apical location (82%). Impairment severity *z*-score was highest for hiatal diameter (3.56) and lowest for vaginal width (1.40). An increase in impairment severity *z*-score was observed with increasing prolapse size among all support sites across all three prolapse size tertiles ( $p < 0.01$  for all).

---

Corresponding author: Christopher X. Hong, Department of Obstetrics and Gynecology, University of Michigan, 1500 E. Medical Center Dr, Ann Arbor, MI 48109, 717-418-5269 (cell), cxhong@med.umich.edu.

Study conducted in Ann Arbor, MI

Manuscript contributions:

CX Hong: Project development, data analysis, manuscript writing

L Nandikanti: Data collection

B Shrosbree: Data analysis

JO DeLancey: Project development, data analysis, manuscript writing

L Chen: Project development, data analysis, manuscript writing

**Conflict of interest summary:** C.X.H. is an advisor/consultant for Cosm Medical, Toronto, ON, Canada. All other authors declare no conflicts of interest.

**Conclusions**—We identified substantial variation in support site failure patterns among women with different degrees of anterior vaginal wall prolapse using a novel standardized framework that quantifies the number, severity, and location of structural support site failures.

## BRIEF SUMMARY

MRI-based structural failure analysis for cystocele revealed remarkable variability between subjects. In general, increased failure frequency and severity are associated with increased prolapse size.

## Keywords

Anterior vaginal wall prolapse; cystocele; hiatus; magnetic resonance imaging; pelvic organ prolapse; structural support site

## INTRODUCTION

Anterior vaginal wall prolapse, or cystocele, is the most common type of pelvic organ prolapse (POP),<sup>1</sup> as well as the most frequent site of operative failure,<sup>2-4</sup> yet our mechanistic understanding of why this type of prolapse occurs and what structural problems are responsible for surgical failure is imperfect.<sup>5</sup> Prior MRI-based studies have shown that anterior vaginal wall prolapse is associated with abnormal pelvic support in specific muscular and connective tissue sites, described as structural “support sites” or “failure sites.”<sup>6</sup> To make progress, a measurement system that assesses the status of each different structural support site is needed.

These support sites can be organized into five support structures grouped into three domains: 1) fibromuscular wall of the vagina (“pubocervical fascia”), characterized by length and width; 2) fascial attachments of the uterus and vaginal wall to surrounding structures, including paravaginal and apical attachments (cardinal/uterosacral); and 3) levator ani muscle injury, which, along with perineal connective tissue damage, results in abnormal hiatal closure.<sup>6</sup> Although there are many different surgical approaches to correct abnormalities presumed to be present at each support site with failure, data concerning the optimal surgical approach for specific types of structural failure or combination of failures remains elusive and prolapse recurrence remains common.<sup>2-4,7,8</sup>

The development of novel 3D MRI measurement strategies have recently allowed for quantitative measurement of structural support site defects in individual women.<sup>6,9</sup> Data from Chen et. al. showed that structural site failures in fascial attachment and hiatal closure were highly correlated and strongly predictive of anterior vaginal wall prolapse presence and size.<sup>6</sup> While this study and others have reported average measurement values for subject groups at specific structural support sites, individual variation in presence and severity of structural support site failure combinations among patients remains unexplored. In addition, the contribution of different failure patterns to different sizes of prolapse is unknown. Understanding patterns in frequency and severity of structural support site failures could, in the future, aid in patient-specific operative planning for choosing the best surgical approach for each type of failure in anterior vaginal wall prolapse repair. The objective of this study

was to develop a standardized framework using stress 3D MRI to compare structural support site failures among women with anterior vaginal wall-predominant prolapse according to increasing prolapse size.

## METHODS

We conducted a cohort study of ninety-one women with anterior vaginal wall-predominant prolapse with uterus *in situ* who had undergone stress 3D MRI as part of prior (n=30)<sup>6</sup> and ongoing (n=61) research studies with the same protocols were selected for this analysis (studies approved by the University of Michigan Institutional Review board: HUM00043445, HUM00031520, HUM00141380, and HUM00138365). All women had symptomatic anterior vaginal wall-predominant prolapse with a pelvic organ prolapse quantification (POP-Q)<sup>10</sup> point Ba at least 1 cm beyond the hymenal ring and point Ba distal or equal to point C in the supine position on clinical exam; a Ba point of +1 cm was chosen to best capture women with symptomatic anterior vaginal wall prolapse outside the normal range of descent in population-based studies of women without prolapse.<sup>11</sup> None of the women had undergone prior pelvic floor reconstructive surgery.

### MRI Acquisition

Stress 3D MRI scans were performed using techniques previously described.<sup>12</sup> Briefly, MRI images in the sagittal and parasagittal planes were acquired in the supine position during maximal Valsalva using a Philips Ingenia 3T scanner with a 15 channel anterior phased array coil. Women were then coached to perform a Valsalva maneuver until they produced a prolapse similar in size to that previously identified during clinical POP-Q examination in the supine position. All Valsalva maneuvers were performed under maximal effort to develop the prolapse, as is done during clinical examination, such that the full extent of the prolapse was revealed. For the stress 3D MRI, women held the Valsalva maneuver for approximately 17 seconds with maximal protrusion of the prolapse as 14 MRI images were obtained in the sagittal plane from one side of the pelvis to the other. The images were reviewed to ensure that the prolapse size visualized on MRI was similar to that obtained from clinical POP-Q examination. Standard anatomic scans at rest were also acquired in the sagittal, coronal, and axial planes using a turbo spin-echo technique. All subjects voided prior to MRI and clinical exam.

### MRI-based Measurements

We used a fiducial-based reconstruction system to identify relevant anatomic points of interest in three-dimensional space. (A fiducial is a marker containing the x, y, and z coordinates of a specific location.) The bony landmarks for the inferior point of the pubic symphysis (arcuate pubic ligament), sacrococcygeal articulation, and ischial spines were identified.

Using the Valsalva MRI scans, an array of fiducials was placed along the anterior vaginal wall and lateral margin using midsagittal and paravaginal slices—thus forming a fiducial “point cloud” representing the 3D shape of the anterior vaginal wall. The anterior fornix, caudal end of the vagina, and five equally spaced sample points along the anterior vaginal

wall (from the anterior fornix to the urethrovaginal junction) were identified using the fiducial point cloud. Bony landmarks were used to perform a rigid transformation of scanner coordinates into coordinates of the modified 3D Pelvic Inclination Correction System (3D PICS),<sup>13</sup> which corrects for differences in subjects' location within the scanner and allows for standardized comparisons between subjects. In the 3D PICS system, the vertical axis (z axis) is aligned with the longitudinal body axis, such that assessments can be made of how high or low pelvic structures lie in the craniocaudal direction relative to the bony pelvis and the direction of gravity when standing.

The anterior vaginal wall length was calculated from the cervicovaginal junction to the distal end of the vagina at the external urethral meatus in the midsagittal plane along the curve of the vaginal wall (Figure 1). Vaginal width was measured at the mid-vagina at the midpoint between the anterior fornix and the urethrovesical junction. The apical location was defined by the craniocaudal position of the anterior fornix, as represented by the 3D PICS z-coordinate. Similarly, paravaginal location was identified as the craniocaudal position of the lateral vaginal wall at the mid-vagina. The diameter of the urogenital hiatus was calculated as the distance between the inferior pubic point and the anterior portion of the perineal body. Prolapse size was defined by the lowest vertical coordinate of the anterior vaginal wall.

### **Standardized Z-Score to compare structural impairment severity within and between patients**

A standardized measurement system was developed to evaluate structural support sites failure in women with anterior vaginal wall prolapse by comparing subject MRI measurements to their respective normal range in women with normal support. First, the mean and standard deviation of MRI measurements for each of the five support sites were calculated to establish the measurement distribution for control subjects based on 30 controls without prolapse in a previously published study with similar protocols.<sup>6</sup> The Shapiro–Wilk normality test showed that structural measurements of 30 control women were normally distributed ( $p > 0.05$  for all measurements). We therefore use sample mean and standard deviation from our control group to estimate the control population distribution and normal range. Then, for each support site in an individual woman, a standardized z-score was calculated relative to the normal distribution in asymptomatic controls without prolapse to determine how her measurements differ from controls, we referred as impairment severity score. For example, a woman's support site with a z-score of 0 would correspond to her measurement equaling the 50th percentile of the measurement distribution in asymptomatic controls. A woman's support site with z-score of 3 is more severely impaired than that of another women with z-score of 1.3. With a z-score system, the severity of different support sites can also be compared, with larger z-score indicating more severe impairment.

### **Failure Frequency Analysis**

In this study, we choose a z-score of 1.28 (corresponding to the 90<sup>th</sup> percentile among controls) as a cutoff score beyond which measurements were considered abnormal. Support site failure frequency was defined as the proportion of z-scores greater than 1.28. We also calculated each structural support site impairment severity z-score and the total impairment

severity score as the mean  $z$ -score for all support sites. Women with prolapse were stratified into three equal tertiles—small, medium, and large—based on increasing prolapse size on MRI and their support site failure frequency and impairment severity were compared.

### Statistical Analysis

Kruskal-Wallis tests and Wilcoxon rank-sum tests were used to compare the failure frequency difference among three tertile groups and post-hoc pair wise comparison. Analysis of variance and standard  $t$ -tests were used for impairment severity score difference among three tertile groups and post-hoc pairwise comparison. Cohen's  $d$  effect sizes were calculated. A  $p$ -value  $<0.05$  was considered statistically significant. All statistics were performed using State version 17.0 (StataCorp LLC, College Station, Texas).

## RESULTS

Demographic characteristics of subjects, stratified into the three size groups, are presented in Table 1. No statistically significant differences were found across the tertiles, except for expected differences in POP-Q measurements. Four women had point Ba equal to point C.

Failure severity, indicated by  $z$ -scores for each of the five support sites, are presented in a color-coded graphic for each subject (Figure 2). There is evident  $z$ -score variation among women with anterior vaginal wall prolapse for each of the five support sites, as demonstrated by the color variation within each column. Each woman also has a unique and varied severity  $z$ -score among all five support sites, as demonstrated by the color variation within each row. In addition, variations in the pattern of support site  $z$ -scores between individual patients is observed, including those with similar prolapse sizes. The number of failed support sites and total severity score for each subject are also presented; this analysis revealed rich patient-specific and structural-specific impairment, despite most of the women in this study having stage 3 prolapse and less varied point Ba on their POP-Q exams.

Among the five support sites, failure frequency was higher among attachment and hiatal support sites compared to vaginal wall support sites (Figure 3). The most common failed support sites were hiatal diameter (91%) and paravaginal location (92%), followed by apical location (82%). Failure frequency was lower for vaginal length (71%) and vaginal width (53%). An increase in failure frequency was observed in all support sites between small and medium/large prolapse size tertiles ( $p<0.01$  for all), but not between medium and large prolapse size tertiles ( $p>0.05$  for all). It is worth noting that vaginal width was the least common failure site overall and that only 29% of women with small prolapse had an abnormally wide vagina. Vaginal width failure frequency approximately doubled for women with medium and large prolapse (68% and 59%, respectively).

Impairment severity  $z$ -score was highest for hiatal diameter (3.56, standard error of the mean [SEM] 0.18) and lowest for vaginal width (1.40, SEM 0.19) (Figure 4). An increase in impairment severity  $z$ -score was observed with increasing prolapse size among all support sites across all prolapse size tertiles ( $p<0.01$  for all support site comparisons), apart from vaginal width between medium and large prolapse size tertiles.

A total impairment severity  $z$ -score was calculated as the mean of the impairment severity  $z$ -score among all support sites. Progression from small, to medium, to large prolapse size tertiles was associated with an increase in the total impairment severity  $z$ -score (small: 1.47, SEM 0.13; medium: 2.60, SEM 0.11; large: 3.60, SEM 0.17,  $p < 0.01$ ). The Cohen's  $d$  effect sizes between small and medium, and medium and large prolapse sizes were 1.65 (95% CI 1.08–2.25) and 1.37 (95% CI 0.81–1.93), respectively. When prolapse size was analyzed as a continuous variable, a strong correlation between prolapse size and total impairment severity  $z$ -score was identified ( $r = 0.81$ ,  $p < 0.01$ , Supplemental Figure 1).

## DISCUSSION

This study introduces a novel standardized framework for evaluating the number, severity, and location of structural support site failures in women with a wide spectrum of anterior vaginal wall prolapse sizes based on a  $z$ -score system with reference to controls subjects without prolapse. We found significant variability in pattern and severity of support site failure between individual women, even those women with same stage and similar size of prolapse. Despite this variability, on average, prolapse progression from small to medium prolapse size is associated with an increase in both the number of support site failures and failure severity, while the difference between medium and large prolapse size is primarily associated with increased severity since almost all sites have failed by this stage of disease. It should be noted, however, that each woman has her own pattern. For example, some women in the large prolapse group have only three support site failures that result in prolapse, while others in the small prolapse group have failures at all five sites that are relatively mild.

A prior study comparing women with cystocele to normal controls using 3D stress MRI showed that apical location, paravaginal location, and urogenital hiatus size were the predominant failure sites and highly correlated with one another.<sup>6</sup> However, the study had to exclude some subjects, particularly those with larger prolapse sizes, due to technical challenges in acquiring MRI sequences at the time, leading to a small sample size ( $n = 30$ ) and possible selection bias.

The findings of the larger prospective cohort are consistent with prior intraoperative observations and MRI studies showing that women with anterior prolapse are more likely to have impairment of attachment and hiatal support sites compared to vaginal wall support sites.<sup>6,14</sup> Data from prospectively recruited subjects confirm and validate the primary support site failures associated with cystocele and their collinearity (Supplemental Figures 2 and 3). Taken together, these studies suggest that cystocele is likely caused by 1) failure of the vagina's apical attachment to the pelvic walls by the cardinal and uterosacral ligaments and paravaginal attachment by abnormal lengthening or avulsion, and 2) an increased genital hiatus area which allows a pressure differential between intraabdominal pressure and atmospheric pressure to act on the vaginal wall, pushing it downward.<sup>12,14,15</sup> Vaginal wall support sites, especially vaginal width, remained the least common structure support sites to fail. Vaginal width failure occurred in less than one-third of women with small prolapse but increased to over half of those with medium to large prolapse, which suggests that vaginal widening is likely a secondary failure.

There is growing consensus that anatomic failure is a biomechanical process; thus, efforts to prevent prolapse formation and operative failure will depend on improved biomechanical understanding of causal mechanisms<sup>16,17</sup> and how they could affect treatment selection. The highlighted patient-specific variability, together with studies investigating structural support after prolapse surgery,<sup>16,18</sup> could help improve understanding of biomechanical mechanisms of prolapse surgery in restoring structural support and prolapse recurrence following surgery.<sup>9,19</sup>

Experienced surgeons are aware that anterior vaginal wall prolapse can take many different forms and that each is unique to the individual.<sup>20</sup> However, there are currently significant disagreements about how to approach these common problems.<sup>21–24</sup> A quantitative framework to identify each individual failure site beyond measuring the vaginal segments that have descended (i.e., POP-Q) has been lacking. Without a conceptual framework and data about the status of each system, it has not been feasible to study how a particular surgical operation performs for a specific structural failure. This research will allow future receiver operator curve analysis to identify evidence-based cutoffs that can predict, for example, which patients with cystocele will have it corrected by sacrocolpopexy alone and who will need concomitant surgery on the anterior wall.

Our findings provide data identifying specific structural support site failures for women with anterior vaginal wall prolapse and a standardized method for determining support site failure severity. The data in our study reveal remarkable variability in the pattern of structural failure for women with cystocele. This variability emphasizes the need and opportunity for personalized surgical planning in the future. Now that patterns in structural site failure can be identified, the outcomes of different surgical strategies for each abnormality can be assessed. In the future, the cost of MRI and alternative strategies such as ultrasound need to be considered before decisions can be made on their routine use in clinical practice. However, has been the case in neurosurgery and orthopedic surgery, imaging has allowed more precise surgical selection and improved surgical care.<sup>25–27</sup> Having evidence for which support sites have and have not failed may allow for more selective surgery, making it feasible to correct specific structural defects during surgery for anterior vaginal wall prolapse.

Historically, assessment of individual prolapse morphology has been largely limited to physical exam and ultrasound findings that measure what has fallen (e.g., anterior wall, apex, posterior wall).<sup>12,20,28</sup> This has been clinically useful in determining what part of the genital tract has fallen and to what degree. Just as the POP-Q measurement system improved the characterization of prolapse by requiring distinction between anterior, posterior, and apical prolapse, this work extends the capability of individualized assessment of anterior vaginal wall prolapse. By providing data on the specific support site failures that are responsible for abnormal vaginal wall displacement that are not measured on POP-Q, including paravaginal height and anterior vaginal wall length and width, this study shifts the paradigm in approach from focusing on “what fell” to “why it fell.”

Although overall patterns in structural failure were identified, statistical characterization of variation within support sites and between patients remains elusive. Several unsupervised

classification methods were attempted to characterize support site failure variability, including hierarchical classification and nearest neighbor k-mean classification using both the standardized *z*-scores and principal components. However, none of these methods led to stable subgroup assignment. It is likely that larger datasets are required to examine patterns in variability using machine learning-based methods, which may uncover patterns in structural site failure that cannot be identified with traditional statistical methods. With further research, it will be possible to re-examine and improve the cutoffs for structural support site failure identification sensitivity and specificity. Now that a scheme is available, this work of improvement can take place.

Based on our findings, it is unlikely there will be one “ideal” surgery for cystocele. With a standardized support site measurement system, the optimal strategy for surgical correction can now be the focus of empirical research rather than case-by-case opinion.<sup>29</sup> The development of surgical planning platforms based on biomechanical models<sup>15,30</sup> may aid in predicting outcomes following different surgical treatment strategies, such as the decision whether to perform a concomitant colpoperineorrhaphy. Indeed, prior studies have identified an enlarged genital hiatus as a risk factor for recurrent prolapse,<sup>31,32</sup> and that correction of an enlarged genital hiatus is associated with a reduction in prolapse recurrence.<sup>33</sup> However, the benefits of a concomitant colpoperineorrhaphy are likely variable between patients and dependent on presence and severity of abnormalities at different structural support sites. In the future, these biomechanical models may be refined and validated to help determine the optimal individualized treatment strategy based on patient-specific structural failure data. Of course, clinical judgement will always be required, but having objective measurements will aid in the clinical decision-making process.

One strength of this study is the relatively large sample size for this type of mechanistic research with the same imaging, measurement protocol, and strategy for all participants. In addition, maximal prolapse size was measured objectively on MRI by an experienced team of investigators. Nonetheless, this study should be interpreted in the context of several limitations. Although this study represents the most comprehensive assessment of different types of pelvic structural support site failure to date, it does not encompass all pelvic support structures (e.g., perineal membrane, deep uterosacral ligament). In addition, although our subjects represented a broad spectrum of anterior vaginal wall prolapse, this study is not population-based and women with large prolapse may be over-represented, as patients referred to our institution often have more advanced prolapse than is typically encountered in general gynecology practice. We also recognize that revising the threshold used to define “failure” may alter the proportion of failure frequency; further work can help improve this issue. However, the relative patterns and variability in structural support site failure are not dependent on the definition of failure. In the future, with a sufficiently large dataset, performing receiver operator curve analysis to establish an evidence-based cutoff for failure will be useful for developing clinical protocols. Finally, the clinical adoption of a *z*-score system to quantify structural site failure may require familiarity by urogynecologists prior to widespread use. However, similar standardized assessment systems, such as the T-score and Z-score system used to interpret results of bone mineral density testing from dual energy X-ray absorptiometry (DEXA) scans, are already widely used in clinical practice.



We have used a novel MRI-based strategy to assess structural support site failures in individual women with anterior vaginal wall-predominant prolapse. Increasing anterior vaginal wall prolapse size is associated with an increase in the number of structural support site failures from small to medium prolapse and an increase in failure severity between all sizes, although significant variation exists between women with similar prolapse sizes. More research is needed to characterize the patterns of support site failure in patients with recurrent anterior vaginal wall prolapse. In the future, considering the unique patterns of pelvic structural failure in individual patients may aid in personalized surgical planning.

## Supplementary Material

Refer to Web version on PubMed Central for supplementary material.

## AWKNOWLEDGEMENTS

The authors thank Sarah Block for assistance in preparing the manuscript.

### Funding:

Supported by National Institutes of Health (NIH) the Eunice Kennedy Shriver National Institute of Child Health and Human Development R01 HD094954, R01 HD038665 and ORWH grant P50 HD044406.

### Presentation:

This study was accepted for oral presentation at the American Urogynecologic Society/International Urogynecology Association Joint Scientific Meeting, June 14-18 2022, Austin, TX

## REFERENCES

1. Olsen AL, Smith VJ, Bergstrom JO, et al. Epidemiology of surgically managed pelvic organ prolapse and urinary incontinence. *Obstet Gynecol.* 1997;89(4):501–506. doi:10.1016/S0029-7844(97)00058-6 [PubMed: 9083302]
2. Weber AM, Walters MD, Piedmonte MR, et al. Anterior colporrhaphy: A randomized trial of three surgical techniques. *Am J Obstet Gynecol.* 2001;185(6):1299–1306. doi:10.1067/mob.2001.119081 [PubMed: 11744900]
3. Nguyen JN, Burchette RJ. Outcome after anterior vaginal prolapse repair: A randomized controlled trial. *Obstet Gynecol.* 2008;111(4):891–898. doi:10.1097/AOG.0b013e31816a2489 [PubMed: 18378748]
4. Shull BL, Bachofen C, Coates KW, et al. A transvaginal approach to repair of apical and other associated sites of pelvic organ prolapse with uterosacral ligaments. *Am J Obstet Gynecol.* 2000;183(6):1365–1374. doi:10.1067/mob.2000.110910 [PubMed: 11120498]
5. Lamblin G, Delorme E, Cosson M, et al. Cystocele and functional anatomy of the pelvic floor: review and update of the various theories. *Int Urogynecol J.* doi:10.1007/s00192-015-2832-4
6. Chen L, Lisse S, Larson K, et al. Structural Failure Sites in Anterior Vaginal Wall Prolapse: Identification of a Collinear Triad. *Obstet Gynecol.* 2016;128(4):853–862. doi:10.1097/AOG.0000000000001652 [PubMed: 27607881]
7. Maher C, Kaven Baessler AE. Surgical management of anterior vaginal wall prolapse: an evidencebased literature review. doi:10.1007/s00192-005-1296-3
8. Weber AM, Walters MD. Anterior vaginal prolapse: Review of anatomy and techniques of surgical repair. *Obstet Gynecol.* 1997;89(2):311–318. doi:10.1016/S0029-7844(96)00322-5 [PubMed: 9015042]
9. Chen L, Swenson CW, Xie B, et al. A new 3D stress MRI measurement strategy to quantify surgical correction of prolapse in three support systems. *Neurourol Urodyn.* 2021;40:1989–1998. doi:10.1002/nau.24781 [PubMed: 34487577]

10. Bump RC, Mattiasson A, Brubaker LP, et al. The standardization of terminology of female pelvic organ prolapse and pelvic floor dysfunction. *Am J Obs Gynecol.* 1996;175:10.
11. Trowbridge ER, Fultz NH, Divya, Patel A, et al. Distribution of pelvic organ support measures in a population-based sample of middle-aged, community-dwelling African American and white women in southeastern Michigan. Published online 2008. doi:10.1016/j.ajog.2008.01.054
12. Larson KA, Luo J, Guire KE, et al. 3D analysis of cystoceles using magnetic resonance imaging assessing midline, paravaginal, and apical defects. *Int Urogynecol J.* 2012;23(3):285–293. doi:10.1007/s00192-011-1586-x [PubMed: 22068322]
13. Reiner CS, Williamson T, Winklehner T, et al. The 3D Pelvic Inclination Correction System (PICS): A universally applicable coordinate system for isovolumetric imaging measurements, tested in women with pelvic organ prolapse (POP). *Comput Med Imaging Graph.* 2017;59:28–37. doi:10.1016/j.compmedimag.2017.05.005 [PubMed: 28609701]
14. DeLancey JOL. Fascial and muscular abnormalities in women with urethral hypermobility and anterior vaginal wall prolapse. *Am J Obstet Gynecol.* 2002;187(1):93–98. doi:10.1067/mob.2002.125733 [PubMed: 12114894]
15. Chen L, Ashton-Miller JA, Delancey JOL. A 3D finite element model of anterior vaginal wall support to evaluate mechanisms underlying cystocele formation. *J Biomech.* 2008;42:1371–1377. doi:10.1016/j.jbiomech.2009.04.043
16. Moalli PA, Bowen ST, Abramowitch SD, et al. Methods for the defining mechanisms of anterior vaginal wall descent (DEMAND) study. *Int Urogynecol J.* 2021;32:809–818. doi:10.1007/s00192-020-04511-1/Published [PubMed: 32870340]
17. Delancey JOL. The hidden epidemic of pelvic floor dysfunction: Achievable goals for improved prevention and treatment. doi:10.1016/j.ajog.2005.02.028
18. Bowen ST, Moalli PA, Abramowitch SD, et al. Defining mechanisms of recurrence following apical prolapse repair based on imaging criteria. doi:10.1016/j.ajog.2021.05.041
19. Chen L, Schmidt P, Delancey JO, et al. Analysis of long-term structural failure after native tissue prolapse surgery: a 3D stress MRI-based study. doi:10.1007/s00192-021-04925-5
20. Brincat CA, Larson KA, Fenner DE. Anterior vaginal wall prolapse: Assessment and treatment. *Clin Obstet Gynecol.* 2010;53(1):51–58. doi:10.1097/GRF.0b013e3181cf2c5f [PubMed: 20142643]
21. Coats E, Agur W, Smith P. WHEN IS CONCOMITANT VAGINAL HYSTERECTOMY PERFORMED DURING ANTERIOR COLPORRHAPHY? A SURVEY OF CURRENT PRACTICE AMONGST GYNAECOLOGISTS. *Int Urogynecol J.* 2010;21:S158–S159.
22. Foon R, Agur W, Kingsly A, et al. Traction on the cervix in theatre before anterior repair: does it tell us when to perform a concomitant hysterectomy? doi:10.1016/j.ejogrb.2011.11.002
23. O’sullivan OE, Matthews CA, O’reilly BA. Sacrocolpopexy: is there a consistent surgical technique? doi:10.1007/s00192-015-2880-9
24. Van Ijsselmuiden MN, Kerkhof MH, Schellart RP, et al. Variation in the practice of laparoscopic sacrohysteropexy and laparoscopic sacrocolpopexy for the treatment of pelvic organ prolapse: a Dutch survey. doi:10.1007/s00192-014-2591-7
25. Norton IH, Orringer DA, Golby AJ. Image-Guided Neurosurgical Planning. *Intraoperative Imaging Image-Guided Ther.* Published online 2014:507–517. doi:10.1007/978-1-4614-7657-3\_37
26. Joskowicz L, Hazan EJ. Computer Aided Orthopaedic Surgery: Incremental shift or paradigm change? *Med Image Anal.* 2016;33:84–90. doi:10.1016/J.MEDIA.2016.06.036 [PubMed: 27407004]
27. Jolesz FA, Golby AJ, Orringer DA. Magnetic Resonance Image-Guided Neurosurgery. *Intraoperative Imaging Image-Guided Ther.* Published online 2014:451–463. doi:10.1007/978-1-4614-7657-3\_32
28. Dietz HP. Ultrasound in the assessment of pelvic organ prolapse. Published online 2018. doi:10.1016/j.bpobgyn.2018.06.006
29. Lensen EJM, Withagen MIJ, Kluivers KB, et al. Surgical treatment of pelvic organ prolapse: a historical review with emphasis on the anterior compartment. doi:10.1007/s00192-013-2074-2
30. Luo J, Chen L, Fenner DE, et al. A multi-compartment 3-D finite element model of rectocele and its interaction with cystocele. doi:10.1016/j.jbiomech.2015.02.041

31. Medina CA, Candiotti K, Takacs P. Wide genital hiatus is a risk factor for recurrence following anterior vaginal repair. Published online 2007. doi:10.1016/j.ijgo.2007.11.008
32. Lowder JL, Oliphant SS, Shepherd JP, et al. Genital hiatus size is associated with and predictive of apical vaginal support loss. Published online 2016. doi:10.1016/j.ajog.2015.12.027
33. Vaughan MH, Siddiqui NY, Newcomb LK, et al. Surgical alteration of genital hiatus size and anatomic failure after vaginal vault suspension. *Obstet Gynecol.* 2018;131(6):1137–1144. doi:10.1097/AOG.0000000000002593 [PubMed: 29742664]

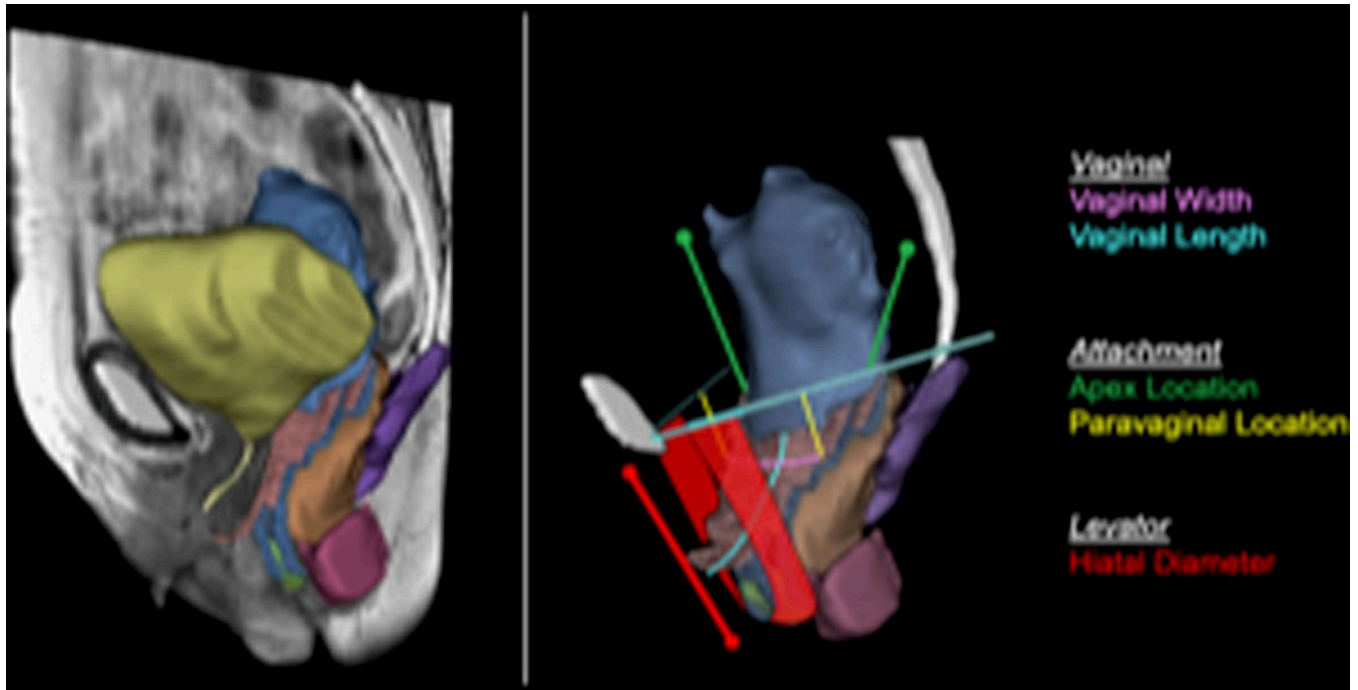


**Figure 1. MRI-based surface model reconstruction of pelvic structures and associated structural support sites.**

Left: Midsagittal MRI slice with 3D surface model reconstruction of relevant anatomic structures. Right: Model with the removal of the MRI slice image and the urinary bladder. The model is labeled with factors that may be abnormal in patients with anterior vaginal wall prolapse, referred to as "support sites". These include two attachment support sites (apex and paravaginal locations), two vaginal wall support sites (vaginal width and length), and one levator support site (hiatal diameter).

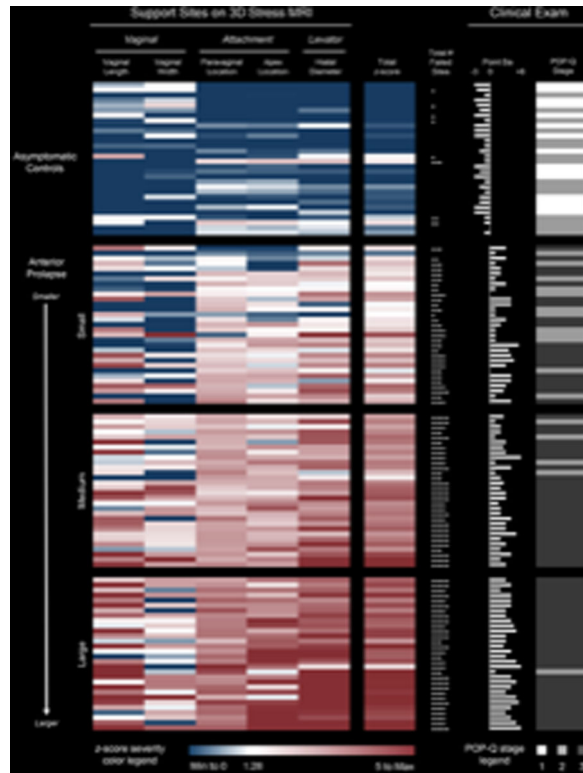


**Figure 2. Heat map constructed using structural support site failure severity z-scores from individual controls and subjects.**

Each participant is represented by a single row. Subjects with symptomatic anterior vaginal wall prolapse are stratified into tertiles based on increasing prolapse size measured on MRI. Rows for asymptomatic controls and anterior prolapse groups are ordered based on prolapse size from smaller prolapse size (top) to larger prolapse size (bottom). Increasing z-score is represented by color shading from blue (normal range) to red (abnormal). White (borderline) is set at a z-score of 1.28, or the 90th percentile among normal controls without prolapse. To allay visual bias, the darkest blue shade was set at z-score of 0, representing the 50<sup>th</sup> percentile among normal controls; with this, negative z-scores appear as the same shade of blue due to similar clinical relevance. The darkest red was set at a z-score of 5 based on the highest impairment severity z-score for the large prolapse group (hiatal diameter); this allowed for greatest visual distinction between the range of abnormal z-scores in the study. The total z-score represents the mean of the impairment severity z-score across all five support sites. The total number of failed support sites is defined by the number of sites with a z-score greater than 1.28.

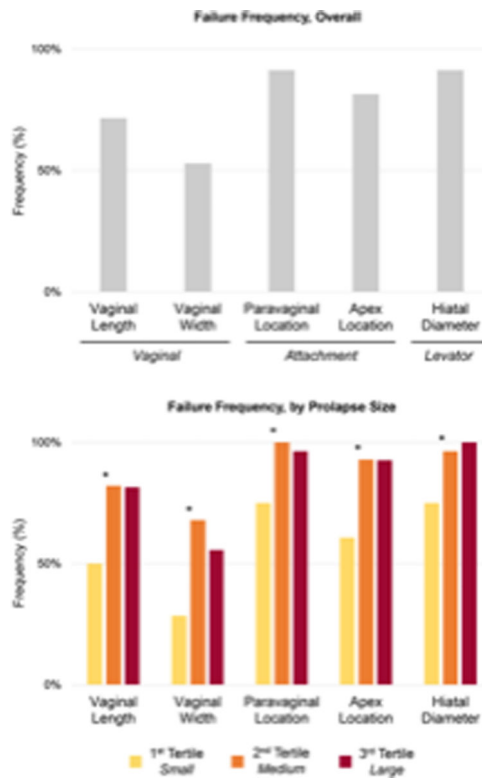


**Figure 3. Structural support site failure frequency**

Top: Structural support site failure frequency among subjects with anterior vaginal wall prolapse (proportion of subjects with an “abnormal” measurement, defined as greater than the 90th percentile of asymptomatic controls without prolapse). Bottom: Structural support site failure frequency among prolapse size tertiles.

\*significant difference in failure frequency between small and medium prolapse size tertiles ( $p < 0.01$ ).

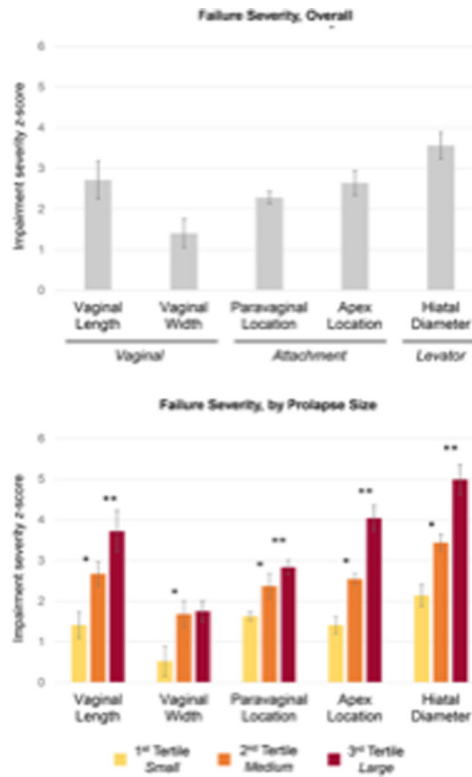


**Figure 4. Structural support site failure severity**

Top: Structural support site failure severity among subjects with anterior vaginal wall prolapse (mean z-score at each failure site). Bottom: Structural support site failure severity among prolapse size tertiles. The effect sizes of pairwise comparisons between groups are presented in Supplemental Table 1.

\*significant difference in failure severity between small and medium prolapse size tertiles ( $p < 0.01$ )

\*\*significant difference in failure severity between medium and large prolapse size tertiles ( $p < 0.01$ ).

Error bars represent standard error of the mean.

**Table 1.**

Demographic characteristics by prolapse size tertiles.

|                              | Small (n=31)     | Medium (n=30)    | Large (n=30)     | p-value |
|------------------------------|------------------|------------------|------------------|---------|
| <b>Age, years</b>            | 57.9 (50.5–67.7) | 62.8 (56.9–67.7) | 63.1 (60.7–67.0) | 0.28    |
| <b>BMI, kg/m<sup>2</sup></b> | 25.9 (23.9–28.0) | 25.0 (22.7–29.2) | 26.1 (23.1–30.7) | 0.83    |
| <b>Parity</b>                | 3.0 (2.0–4.0)    | 3.0 (2.0–3.0)    | 3.0 (2.0–4.0)    | 0.10    |
| <b>POP-Q Point</b>           |                  |                  |                  |         |
| <b>Aa</b>                    | 1.0 (1.0–2.0)    | 1.0 (0.0–2.0)    | 1.0 (1.0–3.0)    | 0.35    |
| <b>Ba</b>                    | 2.5 (1.0–4.0)    | 2.5 (2.0–3.0)    | 4.0 (3.0–5.0)    | <0.01   |
| <b>C</b>                     | –3.0 (–5.0–2.0)  | –3.0 (–4.0–2.0)  | 1.5 (–3.0–4.0)   | <0.01   |
| <b>D</b>                     | –6.0 (–7.5–4.5)  | –6.0 (–8.0–6.0)  | –5.8 (–6.5–5.0)  | 0.03    |
| <b>Ap</b>                    | –2.0 (–2.0–0.0)  | –1.5 (–2.0–0.0)  | –2.0 (–2.0–1.0)  | 0.64    |
| <b>Bp</b>                    | –2.0 (–2.0–0.0)  | –1.5 (–2.0–0.0)  | –2.0 (–2.0–1.0)  | 0.73    |

Data are presented as median (interquartile range)

BMI=body mass index; POP-Q=pelvic organ prolapse quantification